the polymer is reversibly swollen by solvent.[22] For example, the extent of swelling is 5 to 10% by weight when acetonitrile is used.

Self-exchange kinetics were determined for perchlorate using 1 M $LiClO_4$ in water, acetonitrile, and propylene carbonate. The f vs. $t^{1/2}$ plots are given in Figure 8. Diffusion coefficients obtained using eq 5 are $D_{H_2O} = 4.2 \times 10^{-8}$, $D_{ACN} = 3.6 \times 10^{-10}$, $D_{PC} = 3 \times 10^{-13}$ cm^2 s^{-1} in water, acetonitrile, H_2O, and propylene carbonate, respectively. These values may be compared with $D_{H_2O} \sim 2 \times 10^{-8}$ for Cl^- estimated by Burgmayer and Murray[7b] using Cl^- permeation and DC resistance measurements, and D_{ACN} for $ClO_4^- = 2$ to 10×10^{-10} cm^2 s^{-1} obtained by Genies and Pernaut[33] using a potential-step method. The latter result was obtained under conditions where any effect due to electric-field-assisted diffusion would be manifest. The fact that the results are similar to those seen here calls into doubt the importance of the electric field effect in ion transport.

A very strong dependence of diffusion rate on solvent is seen. Since "particle diffusion" is occurring under the conditions used herein (i.e., ion exchange is not limited by solution mass transport), these results imply that the particular solvent that swells the PPy plays a major role in the transport of ions through bulk polymer. Much faster electrochemical "switching"[5a,8] can be expected in aqueous media.

Exchange of Different Ions: Effect on Conductivity. It has often been noted that partially oxidized conducting polymers containing different anions have different conductivities;[34] this has been attributed either to a fundamental effect of the nature of the counterion on conductivity[32a,34b,35] or to the method of partial oxidation of the polymer.[36] Theoretical calculations on the electronic structure of conducting polymers suggest that the geometry of the counterions will have significant effect on electronic conductivity.[37] Ion exchange affords the possibility of rapidly changing the counterion in the same sample of polymer while retaining the same level of partial oxidation of reduction. The above-mentioned effects due to differences in sample preparation can therefore be eliminated.

Preliminary experiments on polypyrrole exchanged with 0.2 M solutions of sodium or potassium salts showed that chloride and fluoride could be exchanged with $^{36}ClO_4$ to 95% completion in 10 min, while larger anions, such as dodecyl sulfate and glutamate, exchanged to an extent of only 10% in the same time. Dichromate, a dianion, did not exchange at all. In all cases the conductivity measured on dried films remained the same (to ±5%) after the exchange regardless of the counterion.

Conclusions

The kinetics of ion exchange in two conducting polymers, polyacetylene and polypyrrole, were determined by self-exchange. Mass transport is limited by diffusion in the exchanging matrix, although the solvent has a strong effect on kinetics. Conducting polymers represent a new class of exchanger with variable capacity possessing the added dimension that the same polymer can be used for exchange in both aqueous systems and organic solvents with a wide range of polarities without the modifications that are necessary for classical ion-exchange resins.[38]

Acknowledgment. This work was supported by a grant from the National Science Foundation.

(33) Genies, E. M.; Pernaut, J. M. *Synth. Met.* **1984/85**, *10*, 117.
(34) (a) Chiang, C. K.; Druy, M. A.; Gau, S. C.; Heeger, A. J.; Louis, E. J.; MacDiarmid, A. G.; Park, Y. W.; Shirakawa, H. *J. Am. Chem. Soc.* **1978**, *100*, 1013. (b) Salmon, M.; Diaz, A. F.; Logan, A. J.; Krounbi, M.; Bargon, J. *Mol. Cryst. Liq. Cryst.* **1982**, *83*, 265.
(35) Hanson, L. K.; Carneiro, K. *Mol. Cryst. Liq. Cryst.* **1985**, *119*, 471.
(36) Druy, M. A.; Rubner, M. F.; Sichel, E. K.; Tripathy, S. K.; Emma, T.; Cukor, P. *Mol. Cryst. Liq. Cryst.* **1984**, *105*, 109.
(37) Bredas, J. L.; Themans, B.; Fripiat, J. G.; Andre, J. M.; Chance, R. R. *Phys. Rev. B.* **1984**, *29*, 6761.
(38) Gregor, H. P.; Hoeschele, G. K.; Potenza, J.; Tsuk, A. G.; Feinland, R.; Shida, M.; Teyssic, Ph. *J. Am. Chem. Soc.* **1965**, *87*, 5525.

Hydrogen Environments in Calcium Phosphates: ^1H MAS NMR at High Spinning Speeds†

James P. Yesinowski* and Hellmut Eckert

Contribution from the Division of Chemistry and Chemical Engineering, California Institute of Technology, Pasadena, California 91125. *Received April 1, 1987*

Abstract: High-resolution ^1H NMR spectra at 200 and 500 MHz of synthetic samples of biologically relevant calcium phosphates have been obtained by using magic-angle spinning (MAS) at spinning speeds up to 8 kHz. The use of high spinning speeds eliminates the need for either isotopic dilution of samples with deuterium or multiple-pulse line-narrowing methods and provides additional structural information, which is absent in the latter two approaches. Structural water molecules in brushite ($CaHPO_4 \cdot 2H_2O$), octacalcium phosphate ($Ca_8H_2(PO_4)_6 \cdot 5H_2O$), and the model compound gypsum ($CaSO_4 \cdot 2H_2O$) yield ^1H MAS NMR spectra with spinning sidebands extending over a 100-kHz range, reflecting the strong, largely inhomogeneous character of the homonuclear dipolar coupling. Structural hydroxyl groups in a series of solid solutions of fluorohydroxyapatites ($Ca_5F_x(OH)_{1-x}(PO_4)_3$) exhibit discrete peaks whose isotropic chemical shift values can be related to different hydrogen-bonding configurations. Surface-adsorbed water molecules in these samples give rise to a resolvable peak; the weakness of the spinning sidebands associated with this peak indicates substantial isotropic mobility of the water protons on the NMR time scale. The isotropic ^1H chemical shifts of protons in calcium phosphates are shown to correlate well with the strength of hydrogen bonding, as measured by O-H···O distances. A linear correlation is observed over a chemical shift range of 0-16 ppm; the accurate data reported here agree remarkably well with ab initio calculations of hydrogen-bonded OH groups reported by Ditchfield and co-workers.

Although calcium phosphates have received much attention in a variety of different disciplines, it is their central role in biomineralization that has provided the major impetus for extensive study of this class of compounds. Calcium hydroxyapatite (HAP, $Ca_5(OH)(PO_4)_3$) is particularly important in this regard, since the mineral phase of mature bone and teeth is believed to be a defect form of hydroxyapatite containing various substitutional impurities. However, other calcium phosphates have been pro-

† Contribution No. 7579.

0002-7863/87/1509-6274$01.50/0

posed as precursors of biological (and synthetic) apatites,[1] including octacalcium phosphate (OCP, $Ca_8H_2(PO_4)_6 \cdot 5H_2O$),[2] OCP–HAP interlayered compounds,[3] amorphous calcium phosphate (typically represented as $Ca_3(PO_4)_2 \cdot xH_2O$),[4,5] and dicalcium phosphate dihydrate ($CaHPO_4 \cdot 2H_2O$).[6,7] The role of these phases in biological mineralization has been the subject of much controversy.[1]

The identification of calcium phosphates in synthetic preparations and mineralized tissue is hampered by their tendency to form nonstoichiometric phases and solid solutions (e.g. with ions such as F^-). One of the most important long-standing structural questions associated with these materials, yet one of the least tractable, is the identification and quantitation of the various forms in which hydrogen atoms occur. The same sample may contain hydrogen in the form of hydroxyl groups, HPO_4^{2-} groups, and H_2O groups, and each of these may be either structural or surface adsorbed. Chemical analysis,[8] thermogravimetry, and spectroscopy have been used to analyze for the presence of these species, but each of these approaches has its limitations. In general, these methods do not distinguish between bulk and surface species, a significant shortcoming in view of the high specific surface area of most apatites. Optical spectroscopy, mainly IR, can provide information about the hydroxyl group in hydroxyapatites[9,10] and fluorohydroxyapatites,[11-14] including the surface hydroxyl groups;[15] however, reliable quantitation is difficult, particularly for the other hydrogen-containing species.

The inherently quantitative nature of the NMR experiment renders it an attractive technique for the structural investigation of calcium phosphates. Previous studies have utilized the favorable NMR properties of ^{31}P and ^{19}F nuclei to obtain quantitative structural information from high-resolution solid-state NMR spectra of calcium phosphates,[16-18] including mineralized tissue. It is therefore somewhat surprising, in view of the innate high sensitivity of ^1H NMR, that high-resolution ^1H NMR studies of calcium phosphates have been reported only recently.[19] Among the small number of low-resolution ("wide-line") ^1H NMR studies of synthetic or biological apatites,[20-26] the only study to identify different hydrogen-containing species utilized the substantial differences in spin–spin relaxation times of the hydroxyl group, structural water, and surface-adsorbed water in dental enamel.[26]

The large range of proton NMR chemical shifts (ca. 20 ppm) observed for oxygen-bound hydrogen in solids,[27] and their sensitivity to hydrogen-bonding effects,[27-29] suggests that high-resolution ^1H NMR should in principle be a very useful technique for studying biologically relevant calcium phosphates. A widely used technique for obtaining high-resolution spectra from solids involves spinning the sample rapidly about an axis making the "magic angle" of 54.7° with respect to the magnetic field (MAS NMR). The main problem encountered with this approach in ^1H NMR is the difficulty of removing the broadening effects of strong homonuclear dipolar couplings among protons. Multiple-pulse line-narrowing techniques combined with MAS[30] or isotopic dilution with deuterium[31] are two approaches that have been successfully used to overcome this problem.

In this paper, we demonstrate that increased spinning speeds (ca. 8 kHz) *alone* can result in highly resolved ^1H MAS NMR spectra. We present here the first high-resolution solid-state ^1H NMR study of calcium phosphates, including hydroxyapatite, fluorohydroxyapatites, calcium monohydrogen phosphate (monetite), calcium monohydrogen phosphate dihydrate (dicalcium phosphate dihydrate, brushite), and octacalcium phosphate.[19] These compounds were selected in an effort to establish the necessary benchmark data required for the investigation of mineralized tissues. A further motivation for this study is to investigate the correlation of the isotropic proton chemical shift with the hydrogen-bonding strength, which has been observed by experimental means[27,28] and in theoretical calculations[29,32] by other workers.

Experimental Section

Sample Preparation and Characterization. The commonly used mineral names for the calcium phosphate samples will be used in this paper, although all samples were synthetic. Hydroxyapatite was prepared hydrothermally and provided by Dr. Jorgen Christoffersen (Medicink-Kemisk Institut, University of Copenhagen, Denmark); its calcium to phosphorus molar ratio of 1.63 is close to the ideal value of 1.67, with the nonstoichiometry being accounted for by both acid phosphates and hydroxyl group vacancies. Further details of its synthesis and characterization are reported elsewhere.[33]

Fluoroapatite was synthesized according to a literature method.[34] The solid solutions of precipitated fluorohydroxyapatites were loaned by Dr. E. C. Moreno of the Forsyth Dental Center, and their preparation[35] and solid-solution character have been previously described.[16]

The sample of monetite, $CaHPO_4$, a gift of Procter and Gamble, had been previously characterized by ^{31}P CP-MAS NMR.[18] Its identity was confirmed again by X-ray powder diffraction using a Guinier camera;

(1) Nancollas, G. H. In *Biological Mineralization and Demineralization*; Nancollas, G. H., Ed.; Dahlem Konferenzen; Springer-Verlag; New York, 1982; pp 79–99. Bonar, L. C.; Grynpas, M. D.; Roberts, J. E.; Griffin, R. G.; Glimcher, M. J. In *The Chemistry and Biology of Mineralized Tissues*; Butler, W. T., Ed.; Ebsco Media, Inc.: Birmingham, AL, 1985; pp 226–233. Brown, W. E.; Chow, L. C.; Siew, C.; Gruninger, S. In *Tooth Enamel IV*; Fearnhead, R. W., Suga, S., Eds.; Elsevier: Amsterdam, 1986; p 8.

(2) Brown, W. E. *Clin. Orthop. Relat. Res.* **1966**, *No. 44*, 205.

(3) Brown, W. E.; Schroeder, L. W.; Ferris, J. S. *J. Phys. Chem.* **1979**, *83*, 1385. Brown, W. E.; Lehr, J. R.; Smith, J. P.; Frazier, A. W. *J. Am. Chem. Soc.* **1957**, *79*, 5318.

(4) Eanes, E. D.; Gillessen, I. H.; Posner, A. S. *Nature (London)* **1965**, *208*, 365.

(5) Termine, J. D.; Posner, A. S. *Calcif. Tissue Res.* **1967**, *1*, 8.

(6) Francis, M. D.; Webb, N. C. *Calcif. Tissue Res.* **1971**, *6*, 335.

(7) Neuman, W. F.; Bareham, B. J. *Calcif. Tissue Res.* **1975**, *18*, 161.

(8) Meyer, J. L.; Fowler, B. O. *Inorg. Chem.* **1982**, *21*, 3029.

(9) Fowler, B. O. *Inorg. Chem.* **1974**, *13*, 194.

(10) Baddiel, C. B.; Berry, E. E. *Spectrochim. Acta* **1966**, *22*, 1407.

(11) Baumer, A.; Ganteaume, M.; Klee, W. E. *Bull. Mineral.* **1985**, *108*, 145.

(12) Freund, F. *Inorg. Nucl. Chem. Lett.* **1977**, *13*, 57.

(13) Freund, F.; Knobel, R. M. *J. Chem. Soc., Dalton Trans.* **1977**, 1136.

(14) Knubovets, R. G.; Kislovskii, L. D. *Tr. Inst. Geol. Geofiz., Akad. Nauk SSSR, Sib. Otd.* **1975**, *No. 50*, 63.

(15) Cant, N. W.; Bett, J. A. S.; Wilson, G. R.; Hall, W. K. *Spectrochim. Acta, Part A* **1971**, *27A*, 425.

(16) Yesinowski, J. P.; Mobley, M. J. *J. Am. Chem. Soc.* **1983**, *105*, 6191. Yesinowski, J. P.; Wolfgang, R. A.; Mobley, M. J. In *Adsorption on and Surface Chemistry of Hydroxyapatite*; Misra, D. N., Ed.; Plenum: New York, 1984; pp 151–175.

(17) Aue, W. P.; Roufosse, A. H.; Glimcher, M. J.; Griffin, R. G. *Biochemistry* **1984**, *23*, 6110. Roufosse, A. H.; Aue, W. P.; Roberts, J. E.; Glimcher, M. J.; Griffin, R. G. *Biochemistry* **1984**, *23*, 6115. Herzfeld, J.; Roufosse, A.; Haberkorn, R. A.; Griffin, R. G.; Glimcher, M. J. *Philos. Trans. R. Soc. London, B* **1980**, *B289*, 459.

(18) Rothwell, W. P.; Waugh, J. S.; Yesinowski, J. P. *J. Am. Chem. Soc.* **1980**, *102*, 2637.

(19) A preliminary account of these results was presented at the Experimental NMR Conference (ENC), Baltimore, MD, April 1986, and published in the Abstracts.

(20) Bhatnagar, V. M. *Technology* **1968**, *5*, 123.

(21) Little, M. F.; Casciani, F. S. *Arch. Oral Biol.* **1966**, *11*, 565.

(22) Myers, H. M.; Myrberg, N. *Acta Odontol. Scand.* **1965**, *32*, 593.

(23) Myers, H. M. *Exp. Cell Res.* **1965**, *38*, 686.

(24) Van der Lugt, W.; Smit, W. A.; Caspers, W. J. *Proc. Colloq. Ampere* **1967**, *14*, 416.

(25) Umezawa, K.; Hiramatsu, M.; Takai, N.; Yamabe, T.; Umezawa, Y.; Nishizawa, T.; Chiba, M. *Bunseki Kagaku* **1975**, *24*, 79–83.

(26) Funduk, N.; Kydon, D. W.; Schreiner, L. J.; Peemoeller, H.; Miljkovic, L.; Pintar, M. M. *Magn. Reson. Med.* **1984**, *1*, 66–75.

(27) Berglund, B.; Vaughan, R. W. *J. Chem. Phys.* **1980**, *73*, 2037–2043.

(28) Jeffrey, G. A.; Yeon, Y. *Acta Crystallogr., Sect. B: Struct. Sci.* **1986**, *B42*, 410.

(29) Rohlfing, C. M.; Allen, L. C.; Ditchfield, R. *J. Chem. Phys.* **1983**, *79*, 4958.

(30) Gerstein, B. C.; Pembleton, R. G.; Wilson, R. C.; Ryan, L. M. *J. Chem. Phys.* **1977**, *66*, 361.

(31) Eckman, R. *J. Chem. Phys.* **1982**, *76*, 2767.

(32) Ditchfield, R.; McKinney, R. E. *Chem. Phys.* **1976**, *13*, 187.

(33) Arends, J.; Christoffersen, J.; Christoffersen, M. R.; Eckert, H.; Fowler, B. O.; Heughebart, J. C.; Nancollas, G. H.; Yesinowski, J. P.; Zawacki, S. J. *J. Cryst. Growth*, in press.

(34) McCann, H. G. *Arch. Oral. Biol.* **1968**, *13*, 987–1001.

(35) Moreno, E. C.; Kresak, M.; Zaradnik, R. T. *Caries Res.* **1977**, *Suppl. 1*, 142.

Table I. ^1H NMR Chemical Shifts in Calcium Phosphates and Gypsum

sample	^1H isotropic chem shift,[a] ppm	assignment
hydroxyapatite (HAP) $Ca_5OH(PO_4)_3$	0.2	structural OH
	1.5 (vw)	OCP defect (?)
	5.5	surface-adsorbed H_2O
	8.7 (vw)	acid phosphate (?)
fluorohydroxyapatite $Ca_5F_{0.24}(OH)_{0.76}(PO_4)_3$	0.3	OH (confign I, Figure 4)
	1.2	H-bonded OH (confign II, Figure 4)
	1.5	H-bonded OH (confign III and IV, Figure 4)
	2.5 (w)	assgnt uncertain
	6.2 (asymm)	surface-adsorbed H_2O
fluorohydroxyapatite $Ca_5F_{0.40}(OH)_{0.60}(PO_4)_3$	0.3	OH (confign I, Figure 4)
	1.4	H-bonded OH (unresolved peaks from confign II–IV, Figure 4)
	2.4 (w)	assgnt uncertain
	6.2	surface-adsorbed H_2O
fluorohydroxyapatite $Ca_5F_{0.81}(OH)_{0.19}(PO_4)_3$	0.4 (sh)	OH (confign I, Figure 4)
	1.6	H-bonded OH (confign III and IV, Figure 4)
	2.5[b] (sh)	assgnt uncertain
	5.9	surface-adsorbed H_2O
fluoroapatite $Ca_5F(PO_4)_3$ (nominal)	1.5 (w)	trace of H-bonded OH (confign III and IV, Figure 4)
	5.8	surface-adsorbed H_2O
monetite $CaHPO_4$	13.6	three acidic proton environments (unresolved)
	16.2	acidic proton most strongly H-bonded
brushite $CaHPO_4 \cdot 2H_2O$	6.4[c]	structural H_2O
	10.4	acidic proton
gypsum $CaSO_4 \cdot 2H_2O$	5.5[c]	structural H_2O
octacalcium phosphate (OCP) $Ca_8H_2(PO_4)_6 \cdot 5H_2O$	0.2	disordered OH (?)
	1.1, 1.5	mobile defect H_2O (?)
	5.5[c]	structural H_2O
	5.5	surface-adsorbed H_2O
	13.0	acidic proton

[a] In ppm from TMS, using secondary references described in Experimental Section. Reproducibility of shifts is estimated to be ±0.1 ppm, except for the (broader) water peaks, which have an estimated reproducibility of ±0.2 ppm. [b] Shift measured by observation of resolved peak in slow-spinning spectrum. [c] Center peak has intense spinning sideband pattern extending over a 100-kHz range.

the 82 reflections observed agreed with those in the ASTM file. Brushite, $CaHPO_4 \cdot 2H_2O$, was obtained commercially from Monsanto Corp.; its identity was confirmed by X-ray powder diffraction, IR spectroscopy, and chemical analysis.

The difficulty of obtaining pure samples of octacalcium phosphate (OCP) is well-known. In the present study, a number of different samples were investigated. Dr. Walter E. Brown, Dr. Ming Tung, and Dr. Branko Tomazic (ADA Health Foundation, NBS) provided several samples of OCP whose identity had been confirmed by X-ray powder diffraction, petrographic microscopy, and calcium and phosphorus chemical analysis.[36] Results are given here for the sample OCP-1, which was prepared by hydrolysis of dicalcium phosphate dihydrate.[37] A second sample of OCP (OCP-2) had been previously characterized by ^{31}P CP-MAS NMR;[18] the presence of OCP in the sample was confirmed after completion of the ^1H MAS NMR experiments by X-ray powder diffraction using a Guinier camera (Cu Kα source) and by FTIR. The diffraction data show the characteristic strong reflection from the OCP d_{100} spacing of 1897 pm (ASTM value 1870 pm). Furthermore, the observed d_{200} spacing of 942 pm (ASTM value 936 pm) and the d_{500} spacing of 376 pm (calculated value[38] 373 pm) indicate that the sample does not contain the type of "intimate" OCP–HAP interlayered phases that exhibit altered d spacings.[38] However, an observed d spacing of 818 pm cannot be assigned to OCP but agrees with the ASTM value for d_{100} of HAP (817 pm). (The latter reflection is the only strong one that can be used unequivocally to identify HAP in the presence of OCP.) On this basis we conclude that some HAP has formed in the OCP sample via solid-state conversion; if OCP-HAP interlayers are formed, the individual layers must be more than a few unit cells thick, since they diffract independently. In addition, all of the strong reflections listed for $CaHPO_4$ (monetite) in the ASTM file are observed in this sample. In agreement with the X-ray results, FTIR spectra in the range 400–4000 cm^{-1} confirm the presence of OCP as the major component in sample OCP-2, but peaks at 630 and 3572 cm^{-1} suggest the presence of some hydroxyapatite (monetite does not exhibit major IR peaks that clearly distinguish this compound from the other phases present[39]). These results suggest that the following solid-state disproportionation reaction has consumed some of the OCP: $Ca_8H_2(PO_4)_6 \cdot 5H_2O = 3CaHPO_4 + Ca_5(OH)(PO_4)_3 + 4H_2O$. While transformation of OCP to monetite and HAP has been previously reported to occur at elevated temperatures (180–220 °C),[3] we believe that this is the first report of such a transformation occurring at ambient temperature.

Nuclear Magnetic Resonance Studies. The initial ^1H MAS NMR experiments were carried out at 200 MHz on a home-built spectrometer, equipped with a magic-angle spinning CP-MAS probe from Doty Scientific, Inc., and 7-mm-o.d. sapphire rotors capable of spinning up to 5 kHz. Subsequent experiments employed two ^1H MAS NMR probes from Doty with 5-mm-o.d. sapphire rotors (sample volume ca. 0.1 cm^3), which are capable of spinning at higher (8-kHz) speeds and were designed for low proton background signal. The spectra were obtained on the home-built 200-MHz spectrometer and/or a Bruker WM-500 spectrometer. The ^1H 90° pulse lengths were 2–4 μs at 200 MHz and 8 μs at 500 MHz. A 5-mm nonspinning tube of ethanol was used to optimize the field homogeneity and to reference the hydroxyl chemical shift in HAP (the methyl group chemical shift was set to 1.11 ppm from TMS). The HAP sample was subsequently used as a secondary chemical shift reference, in order to improve the reproducibility of the chemical shift measurements (±0.1 ppm). The commercial availability of HAP, the narrow line width of the hydroxyl resonance ($\Delta\nu_{1/2}$ = 200 Hz), and its favorable intensity and relaxation times make HAP an ideal reference compound for ^1H MAS NMR studies: It provides a secondary chemical shift reference, can be used to adjust the magic-angle, and can be used to shim the magnetic field with a spinning sample. For some samples, spin-lattice relaxation times were measured with use of the inversion–recovery null-point method; the range observed for the peaks in $Ca_5(PO_4)_3F_{0.24}(OH)_{0.76}$ was 140 ms to 1.2 s and was typical of the reasonably short T_1 values for these samples. Therefore, the MAS NMR spectra were readily obtained under nonsaturating conditions. The free-induction decays were multiplied by an exponential apodization function, equivalent to a Lorentzian line broadening of 10–20 Hz, and were zero-filled from 2K to 8K data points prior to Fourier transformation. The curved base line observed in several spectra is presumably due to a delayed receiver recovery. Left-shifting and base-line fitting were not used due to their subjective character.

Results and Assignments

Table I lists the chemical shifts of all of the resolved peaks observed in the compounds under investigation and the proposed assignments. In the following sections, we will discuss these

(36) Brown, W. E., personal communication.
(37) Tung, M.; Brown, W. E. *J. Dent. Res.* **1985**, *64*, 2.
(38) Brown, W. E.; Schroeder, L. W.; Ferris, J. S. *J. Phys. Chem.* **1979**, *83*, 1385.
(39) Petrov, I.; Soptrajanov, B.; Fuson, N.; Lawson, J. R. *Spectrochim. Acta, Part A* **1967**, *23A*, 2637.

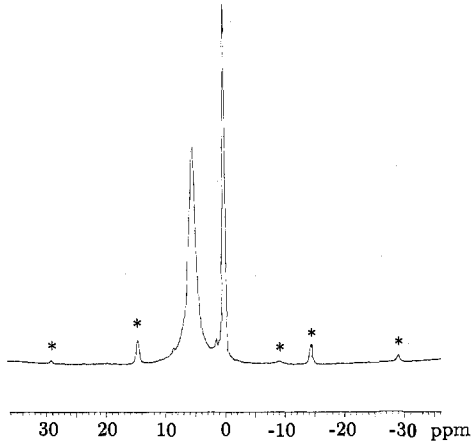

Figure 1. ^{1}H MAS NMR spectrum of hydroxyapatite ($Ca_5(OH)(PO_4)_3$) at 500.13 MHz (spinning speed 7.3 kHz). Spinning sidebands are indicated by an asterisk.

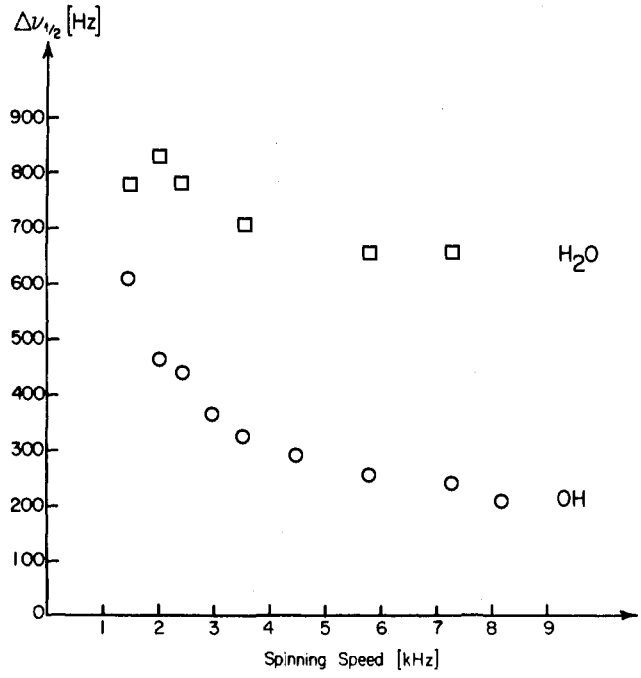

Figure 2. 500.13-MHz ^{1}H MAS NMR line widths of the OH and the H_2O peaks in hydroxyapatite versus spinning speed.

assignments in terms of the crystallographic and spectroscopic information available in the literature.

$Ca_5(OH)(PO_4)_3$ (Hydroxyapatite). The 500-MHz ^{1}H MAS NMR spectrum of hydroxyapatite is shown in Figure 1. At first glance, the observation of two well-resolved resonances seems surprising in view of the crystal structure of HAP,[40] which contains linear chains of structurally equivalent hydroxide ions parallel to the *c* axis. However, thermogravimetric analyses have shown that apatites of colloidal dimensions (such as the sample studied here) contain a significant amount of surface-adsorbed water.[33] We assign the peak at ca. 5.6 ppm in Figure 1 to this species, since it is not observed in samples with significantly lower surface areas.[41] Further confirmation of this assignment is given by the observation that the intensity of this peak decreases upon exchange with D_2O in the vapor phase. The ability to selectively replace the surface H_2O groups with D_2O provides a convenient method of reducing the signal intensity from adsorbed species and may

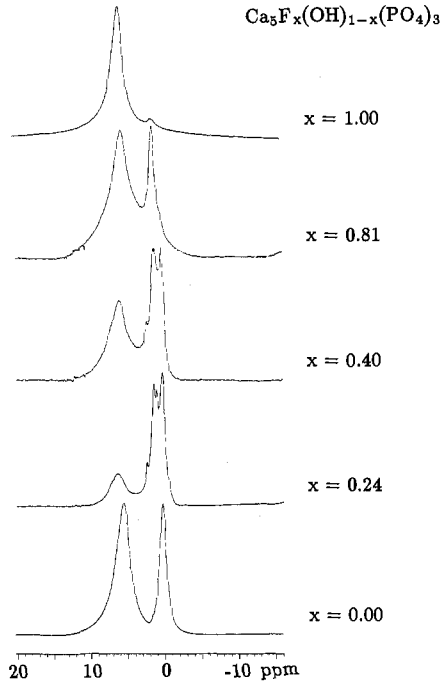

Figure 3. ^{1}H MAS NMR spectra at 200.27 MHz of fluorohydroxyapatites ($Ca_5F_x(OH)_{1-x}(PO_4)_3$). Spinning speeds are 4.5–5 kHz.

be useful when searching for additional weaker resonances in defect apatite samples.

The structural hydroxyl group in HAP resonates at 0.2 ppm, the highest upfield value observed for these samples and upfield of the 2.0–4.6 ppm shift range reported for hydroxyl groups in other solids.[42] This extremely high upfield shift value reflects very weak hydrogen bonding, as evidenced by the O–H stretching frequency in the IR (3572 cm^{-1}).[15] It should be pointed out that the O–H···O distance along the *c* axis (344 pm) may be too long for hydrogen bonding; in order to account for correlations of the O–H stretching frequency with O–O distances, it has been proposed that a bent hydrogen bond to a phosphate oxygen may form, with an O–H···O distance of 307 pm.[10] Figure 2 demonstrates that the hydroxyl resonance in HAP narrows with an increase in the spinning speed but is, nevertheless, reasonably sharp even at spinning speeds as low as 1.5 kHz. The presence of a linear chain of homonuclear spins, as found in HAP, has been predicted to result in a dipolar interaction that is inhomogeneous in the MAS NMR sense.[43] This fact, along with the relatively weak magnitude of the other dipolar interactions, undoubtedly contributes to the favorable line-narrowing characteristics observed.

Two very small peaks at 1.5 and 8.7 ppm are apparent in Figure 1. The first peak may arise from the presence of OCP in central planar defects, one unit cell thick, as has been recently proposed by Nelson et al. in synthetic carbonated apatites,[44] or from OCP unit cells on the surface. The peak at 8.7 ppm can be assigned to small amounts of HPO_4 groups, which are known to be present in this sample at low levels.[33]

It is interesting to note that surface hydroxyl groups in HAP have been assigned to a stretching frequency of 3660 cm^{-1} in the IR,[15] indicative of little or no hydrogen bonding. We do not observe any peaks upfield from the 0.2 ppm OH peak in HAP, even though the specific surface area of the sample (37 m^2/g)[33] suggests the presence of a significant fraction of hydroxyl groups at the surface. The surface hydroxyl resonance may not be resolved from that of the bulk hydroxyls, or it may be in rapid chemical exchange with the surface-adsorbed water.

(40) Kay, M. I.; Young, R. A.; Posner, A. S. *Nature (London)* **1964**, *204*, 1050.
(41) Yesinowski, J. P.; Eckert, H.; Holcomb, D.; Young, R. A., to be submitted for publication.
(42) Ratcliffe, C. I.; Ripmeester, J. A.; Tse, J. S. *Chem. Phys. Lett.* **1985**, *120*, 427–32.
(43) Maricq, M. M.; Waugh, J. S. *J. Chem. Phys.* **1979**, *70*, 3300.
(44) Nelson, D. G. A.; Wood, G. J.; Barry, J. C.; Featherstone, J. D. B. *Ultramicroscopy* **1986**, *19*, 253.

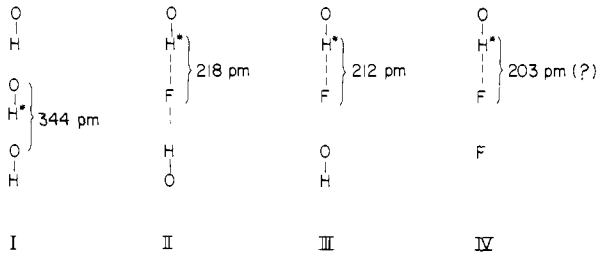

Figure 4. Hydroxyl group configurations and NMR-derived distances[46,49] along the crystallographic c axis in fluorohydroxyapatites. The distance given for IV is believed to be less accurate (see text). The O–O distance in configuration I is obtained from the HAP crystal structure.[40]

Fluorohydroxyapatites. The ^{1}H MAS NMR spectra of the three fluorohydroxyapatite samples and the sample of fluoroapatite are shown in Figure 3. In concordance with the results on HAP, we assign the broad peak observed at 5.8–6.3 ppm in these samples to surface-adsorbed water. Fluoroapatite is isostructural with HAP,[45] enabling the formation of solid solutions of fluorohydroxyapatites. The presence of fluorine causes perturbations of the hydrogen environments, involving some displacement of both fluoride and hydroxyl groups from their normal positions due to hydrogen bonding, as discussed below. The most upfield peak at 0.3–0.4 ppm is assigned to the unperturbed structural hydroxyl group, since it is most intense in the high hydroxide concentration samples and its shift is not significantly different from the corresponding peak in HAP at 0.2 ppm. In addition, several resonances between 1.2 and 2.5 ppm are observed, reflecting perturbations of the hydrogen environment caused by the presence of fluorine. Single-crystal NMR studies of natural minerals[46-49] have provided values for the hydrogen–fluorine distances in fluorohydroxyapatites that are indicative of weak hydrogen bonding between the hydroxyl and the fluoride. Figure 4 summarizes the distance data for various configurations along the linear chain of fluoride and hydroxide ions. A stronger hydrogen bond is formed when the fluoride is only singly hydrogen bonded (III and IV) rather than doubly hydrogen bonded (II). The difference in the distances between III and IV seems unreasonable from a structural standpoint and is not predicted from the interpretation of the IR and ^{1}H MAS NMR results discussed in the following paragraph. We believe that the distances for II and III, derived from the dipolar coupling constants measured by ^{1}H NMR, are more accurate than the one for IV derived from ^{19}F NMR, since only the former analysis involves isolated spin pairs.

IR studies of fluorohydroxyapatites[11-14] show two O–H stretching bands with maxima near 3547 and 3541 cm^{-1}, which have been assigned[11] to doubly hydrogen-bonded groups (configuration II) and singly hydrogen-bonded groups, respectively. Although configuration IV was the only one considered for the 3541-cm^{-1} band in ref 11, we believe that the hydrogen-bonded hydroxyl in configuration III observed in the single-crystal NMR studies should yield a similar hydroxyl stretching frequency. We therefore propose the following interpretation of the ^{1}H MAS NMR results, which closely matches this interpretation of the IR results and agrees with the compositional dependencies of the peaks and the predicted downfield shifts due to stronger hydrogen bonding. The peak at 1.5–1.6 ppm in the various samples is assigned to the singly hydrogen-bonded configuration IV, since it is most pronounced in the fluorohydroxyapatite sample with the lowest hydroxide concentrations (19%), and is also the only hydroxyl peak seen (in trace amounts) in the FAP sample. The singly hydrogen-bonded configuration III also resonates at 1.5 ppm, since this peak is also seen in the fluorohydroxyapatite with the highest hydroxide concentrations (76%), where IV is unlikely to occur. The peak at 1.2 ppm is assigned to configuration II, since it is only distinctly observed in the highest hydroxide concentration sample (76%); it is slightly upfield of the 1.5 ppm peak since the hydrogen bond is slightly weaker. The relative sideband intensities (data not shown) observed for the hydroxide protons in configurations II–IV are significantly greater than those associated with the peak at 0.3–0.4 ppm, due to the large (and inhomogeneous) proton–fluorine dipolar coupling.

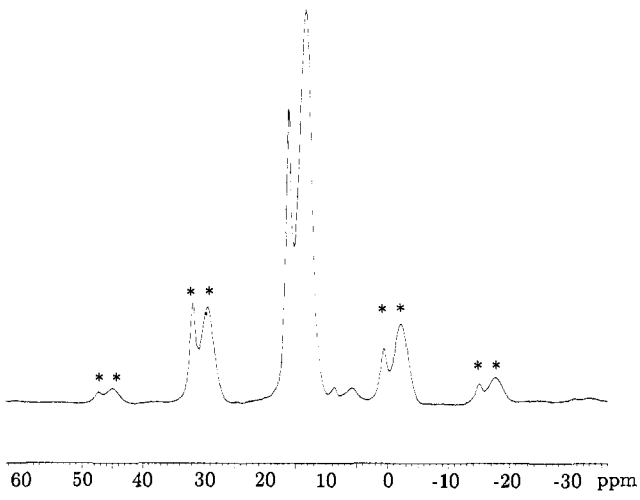

Figure 5. ^{1}H MAS NMR spectrum at 500.13 MHz of monetite, $CaHPO_4$. Spinning speed is 7.9 kHz. Spinning sidebands are indicated by an asterisk. The weak peaks between 5 and 9 ppm are presumably due to impurities.

The peak at 2.5 ppm, which is observed in the three fluorohydroxyapatite samples, is difficult to assign. The fact that this peak remains sharp at spinning speeds as low as 0.5 kHz and does not give rise to any discernible sidebands suggests a highly mobile "structural water" group such as has been observed in ^{2}H NMR of deuteriated apatites.[41] Confirming the interpretation of previous ^{19}F NMR results,[16] these ^{1}H MAS NMR results are consistent with the solid-solution character of the samples studied. The observation of the 0.3–0.4 ppm peak due to hydroxyls *not* hydrogen bonded to fluoride in all three samples supports the statistical mixing of fluoride and hydroxide inferred from IR results,[11] rather than a scheme that maximizes the hydrogen bonding between fluoride and hydroxide. The latter scheme would predict that all hydroxyl groups should form hydrogen bonds to fluoride below a level of 50% hydroxide, contrary to our results. While ordering has been inferred for fluorohydroxyapatite samples annealed at 250 °C for 300 h,[12,13] the present samples, formed by aqueous precipitation, are presumably more likely to have a statistical distribution that is kinetically "frozen in".

$CaHPO_4$ (Monetite). Several crystallographic studies of monetite have been carried out,[50-52] since the structural details involving the proton positions have proven controversial and/or ambiguous. Part of the difficulty may stem from the existence of an order–disorder transition near room temperature between two forms, a low-temperature P1 phase and a high-temperature disordered P$\bar{1}$ phase.

Figure 5 shows the ^{1}H MAS NMR spectrum of monetite, $CaHPO_4$, indicating two clearly distinguishable hydrogen environments. It is possible to interpret the observation of two peaks in the spectrum with an intensity ratio of approximately 1:3 in

(45) Naray-Szabo, St. *Z. Kristallogr., Kristallgeom., Kristallphys., Kristallchem.* **1930**, *75*, 387. Beevers, C. A.; McIntyre, D. B. *Mineral. Mag. J. Mineral. Soc.* **1944–1946**, *27*, 254.

(46) Van der Lugt, W.; Knottnerus, D. I. M.; Perdok, W. G. *Acta Crystallogr., Sect. B: Struct. Crystallogr. Cryst. Chem.* **1971**, *B27*, 1509.

(47) Knoubovets, R. G.; Afanasjev, M. L.; Gabuda, S. P. *Spectrosc. Lett.* **1969**, *2*, 121.

(48) Young, R. A.; Van Der Lugt, W.; Elliott, J. C. *Nature (London)* **1969**, *223*, 729.

(49) Vakhrameev, A. M.; Gabuda, S. P.; Knubovets, R. G. *J. Struct. Chem. (Engl. Transl.)* **1978**, *19*, 256.

(50) Dickens, B.; Bowen, J. S.; Brown, W. E. *Acta Crystallogr., Sect. B: Struct. Crystallogr. Cryst. Chem.* **1971**, *B28*, 797.

(51) Catti, M.; Ferraris, G.; Filhol, A. *Acta Crystallogr., Sect. B: Struct. Crystallogr. Cryst. Chem.* **1977**, *B33*, 1223.

(52) Catti, M.; Ferraris, G.; Mason, S. *Acta Crystallogr., Sect. B: Struct. Crystallogr. Cryst. Chem.* **1980**, *B36*, 254.

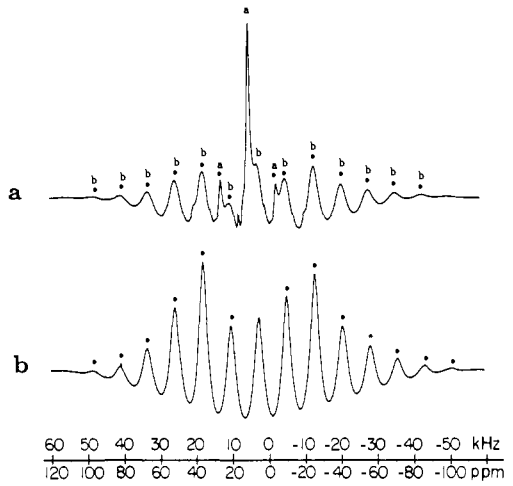

Figure 6. ^{1}H MAS NMR spectra at 500.13 MHz: (a) brushite, $CaHPO_4 \cdot 2H_2O$; spinning speed 7.6 kHz; labels a and b refer to central peaks and spinning sidebands (with asterisks) of the acidic proton and water molecules, respectively. (b) gypsum, $CaSO_4 \cdot 2H_2O$; spinning speed 7.7 kHz.

terms of the crystallographic data by considering only the strength of hydrogen bonding, as reflected by the O–O distance, and ignoring the question of proton disordering in the high-temperature phase (presumably present in our sample). Thus, both X-ray and neutron diffraction identify the strongest "quasi-symmetric" hydrogen bond as being a nearly linear one between O(7) and O(7′) (notation of ref 50), with the O–O distance being between 246 and 248 pm. We assign the corresponding hydrogen, H(1), to the downfield peak at 16.2 ppm in the MAS NMR spectrum. There are two centrosymmetrically related, nearly linear, hydrogen bonds between O(1) and O(5′), with O–O distances of 256 pm. We assign the corresponding two equivalent hydrogens, H(2), to the upfield peak at 13.6 ppm in the MAS NMR spectrum. The remaining hydrogen bond, which is statistically disordered in the high-temperature phase, fills half of the sites between O(6) and O(8′). X-ray studies indicate an average O–O distance of 267 pm for this site.[50] Taking into account the statistical disorder and excess thermal vibrational amplitudes, the authors estimated the actual O–H···O bond length to be 259 pm. The corresponding proton, H(3), is also assigned to the upfield peak at 13.6 ppm in the MAS NMR spectrum and is presumed to be unresolved from the H(2) protons.

$CaHPO_4 \cdot 2H_2O$ (Brushite) and $CaSO_4 \cdot 2H_2O$ (Gypsum). The hydrogen atom positions in brushite have been established in a single-crystal neutron diffraction study.[53] The structure contains two water molecules with distinctly different hydrogen-bonding characteristics: Water (1) has two moderately strong, nearly linear hydrogen bonds to phosphate oxygens of the O(3) type, while water(2) has less linear hydrogen bonds, one of which is unusually long. The O–H···O distances of 276 and 278 pm (water(1)) and 283 and 309 pm (water(2)) correlate well with distinct absorption bands observed by infrared spectroscopy.[54] The acidic hydrogen atom bridges two oxygens of neighboring phosphate tetrahedra, thus forming a nearly linear hydrogen bond with an O–H···O distance of 268 pm. From wide-line ^{1}H NMR experiments the dipolar line width (square root of the second moment) of the anionic hydrogen atom has been estimated to be ca. 8 kHz, consistent with a location in the crystal structure rather remote from the water molecules.[55]

Figure 6a shows the ^{1}H MAS NMR spectrum of brushite. In our experiments, performed at a spinning speed of ca. 8 kHz, typical MAS NMR peak patterns of two distinct hydrogen species can be resolved, which are labeled a and b. Pattern a consists of a strong centerband at 10.4 ppm, flanked by two pairs of weaker spinning sidebands, while pattern b shows a centerband at 6.4 ppm, with a set of much stronger spinning sidebands extending over a 100-kHz range. The relative areas associated with these peak patterns (approximately 1:4) suggest the assignment of pattern a to acidic protons and of pattern b to molecular hydrate water. This assignment is further confirmed by inspection of Figure 6b, which shows that the hydrate water molecules of the structurally closely related[56] compound gypsum, $CaSO_4 \cdot 2H_2O$, give rise to a ^{1}H MAS NMR peak pattern very similar to pattern b in the spectrum of brushite. Furthermore, the assignment given above is consistent with the fact that the acidic hydrogen atom in brushite participates in a shorter hydrogen bond than the water molecules. However, the four different hydrogen-bonding environments for the hydrate water in brushite[53] are not clearly resolved in the spectrum at the spinning speed used. (The shoulder on the upfield side of the MAS centerband assigned to the hydrate water molecules suggests that the resonance due to the long hydrogen bond of water(2) is partly resolved. Since, however, no accurate chemical shift can be extracted for this resonance, this point has not been included in the chemical shift correlation discussed below.)

$Ca_8H_2(PO_4)_6 \cdot 5H_2O$ (Octacalcium Phosphate). The single-crystal X-ray diffraction study[57] of OCP reveals a structure composed of an "apatitic layer" and a "water layer". The apatitic layer has an arrangement of calcium and phosphate ions very close to that in HAP, with both a phosphate oxygen and a water oxygen taking the place of the (two) hydroxyl groups present in the HAP structure (see, however, below). The water layer is an irregular channel filled with molecules of hydration. In that study, partial occupancy of one of the water sites was observed, but it was assumed that full occupancy, which was crystallographically feasible, would result in an ideal stoichiometry of $Ca_8H_2(PO_4)_6 \cdot 5H_2O$. A recent X-ray diffraction refinement of the OCP structure[58] shows one of the acidic protons (H(2)) to be located between two phosphate units, with an O–H···O distance of 247.7 pm (the numbering of ref 58 is used, which differs from that in ref 57). The other acidic hydrogen atom position (H(1)) is proposed to occur within the hydrated layer between a phosphate group and a structural water molecule (O–H···O distance 272.6 pm), but this assignment is complicated by positional disordering.

The ^{1}H MAS NMR spectrum of sample OCP-1, shown in Figure 7a,b, reveals substantial complexity. The correlation of ^{1}H NMR chemical shifts with O–H···O bond distances (see below) suggests assignment of the peak at 13.0 ppm to H(2), whereas the resonance due to H(1) is not clearly resolved, presumably because of the positional disorder mentioned above and overlap with the resonances assigned to structural water (see below).

Parts a and c of Figure 7 show, in addition, a spinning sideband pattern centered around 5.5 ppm typical of the patterns of crystalline hydrate water discussed above. The intensity of the centerband at 5.5 ppm relative to the spinning sidebands is considerably greater than that observed for brushite or gypsum (see Figure 6a,b). We attribute this to a superimposed resonance arising from more mobile water species, which could be either surface-adsorbed or structurally incorporated. The recent structure refinement[58] yields a number of different O–O distances for the hydrate water molecules, but such differences are not resolved in the ^{1}H MAS NMR spectrum.

Furthermore, two distinct peaks are observed at 1.1 and 1.5 ppm. Both peaks are unusual in that they remain sharp down to very low spinning speeds (0.5 kHz), where they show relatively intense spinning sidebands, while the other peaks in the spectrum are greatly broadened. This observation suggests that these peaks arise from water molecules undergoing rapid reorientation on the NMR time scale at room temperature. (Further evidence of molecular motion in OCP has already been given by previous variable-temperature ^{31}P MAS NMR[18] and nonspinning ^{1}H NMR experiments.[59]) The most plausible assignment of these two peaks

(53) Curry, N. A.; Jones, D. W. *J. Chem. Soc. A* **1971**, 3725.
(54) Casciani, F.; Condrate, R. A., Sr. *Spectrosc. Lett.* **1979**, *12*, 699. Berry, E. E.; Baddiel, C. B. *Spectrochim. Acta, Part A* **1967**, *23A*, 2089.
(55) Jones, D. W.; Smith, J. A. S. *Trans. Faraday Soc.* **1960**, *56*, 638.
(56) Atoji, M.; Rundle, R. E. *J. Chem. Phys.* **1958**, *29*, 1306.
(57) Brown, W. E.; Smith, J. P.; Lehr, J. R.; Frazier, A. W. *Nature (London)* **1962**, *196*, 1048.
(58) Mathew, M.; Brown, W. E.; Dickens, B.; Schroeder, L. W., in press.

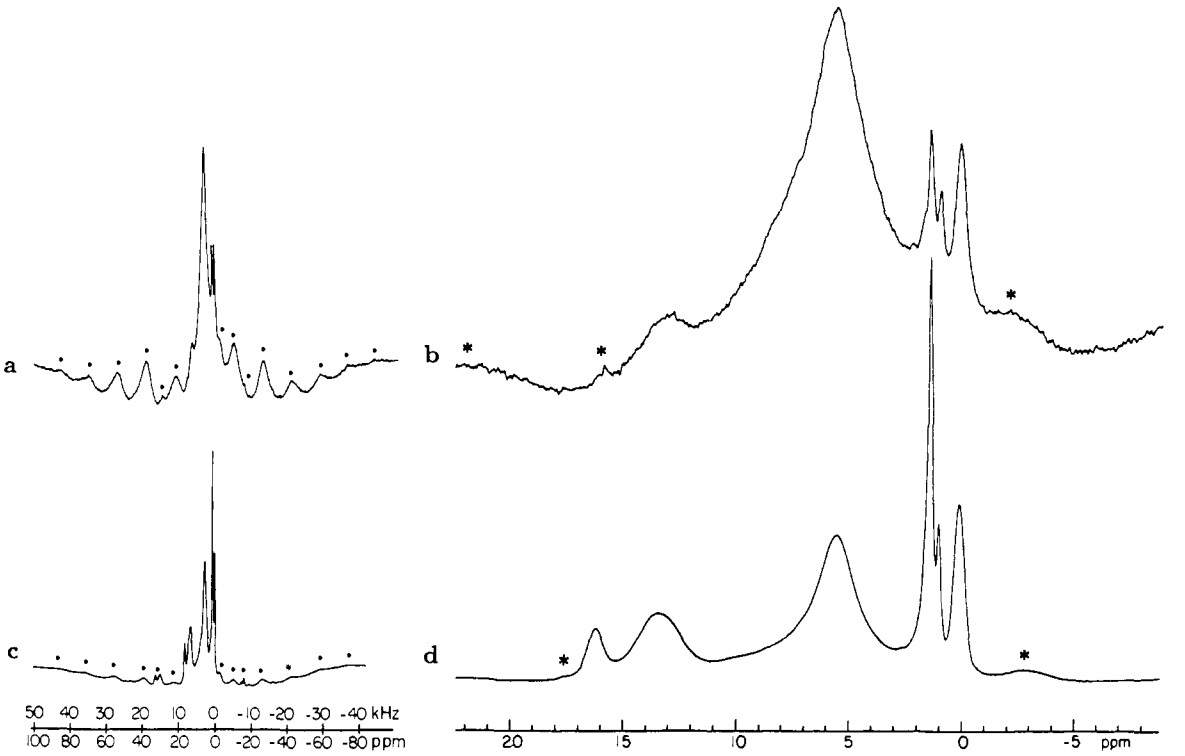

Figure 7. ^{1}H MAS NMR spectra at 500.13 MHz of octacalcium phosphate ($Ca_8H_2(PO_4)_6 \cdot 5H_2O$) samples. Spinning sidebands are indicated by asterisks. Key: (a) sample OCP-1, spinning speed 7.8 kHz; (b) expanded plot of spectrum in 7a; (c) sample OCP-2, spinning speed 8.2 kHz; (d) expanded plot of spectrum in 7c.

is to the O(5) water molecule (O-43 in ref 57), which is isolated from the other water molecules in the OCP structure and for which the X-ray data indicate disorder as well as large thermal vibrational amplitudes. The upfield location of these peaks is consistent with the large O–O distances reported for this water molecule.[58] Among the different samples studied, a great variability in the intensities of these peaks can be noted, indicating that this mobile water species may not be present in stoichiometric amounts. This can be understood in terms of the "zeolitic" nature of the hydrate water of OCP, which is liberated continuously upon heating from room temperature to 600 °C.[60]

As discussed further by Brown,[58] the possibility of a hydrogen redistribution according to the formula $Ca_{16}H_{4+x}(PO_4)_{12}(OH)_x \cdot (10 - x)H_2O$ ($0 < x < 2$) not only introduces additional possibilities for positional disorder but also implies the formation of OH groups. The most likely location of these OH groups[58] is the O(4) site (O(42) in ref 57) in the apatitic layer, which is nearly identical with the site for OH in HAP. Both OH and H_2O groups may occupy this site in statistical disorder. In this connection, we note that a peak at 0.2 ppm is seen in all of the OCP samples we have studied. This chemical shift is identical with that of the hydroxyl group in HAP, and the line width and spinning sideband intensities associated with this peak closely match those observed in HAP. Although in principle this peak could also arise from an impurity of HAP, neither FTIR, X-ray powder diffraction data, nor the Ca/P ratio indicates the presence of such a phase. Thus, by establishing the presence of OH groups in the "apatitic layer", the NMR data are in support of the proposal of Brown and co-workers[58] that OCP is even more closely related to HAP than considered previously.

Parts c and d of Figure 7 show the spectrum of OCP-2. Both the extensive spinning sideband pattern associated with the hydrate water molecules and the three sharp upfield peaks identified in Figure 7a,b are clearly visible in this spectrum. The results given in the Experimental Section show that this sample had undergone a partial solid-state transformation to monetite and HAP. Figure 7d illustrates the power of ^{1}H MAS NMR to resolve a variety of different hydrogen environments in a multiphase sample. The monetite component and the different water groups are fairly well resolved, whereas the HAP component is superimposed upon the peak at 0.2 ppm assigned to the disordered OH in the OCP structure.

Discussion

The following discussion deals with the structural and dynamical information contained in the MAS NMR spectra, as well as with the correlation of isotropic chemical shifts with hydrogen-bonding strengths.

Surface-Adsorbed Water. Surface-adsorbed water represents a major part of the hydrogen content in apatites of colloidal dimensions. The differential heat of adsorption of water on synthetic hydroxyapatite degassed at 450 °C ranges from 23 kcal/mol for the lowest coverage to approximately 11 kcal/mol for coverages above two monolayers, at which point additional adsorbed water condenses onto a "liquid-like" layer.[61] The line width (full width at half-height) of the peak assigned to surface-adsorbed water is 1100 Hz for the static HAP sample at 200 MHz, whereas it is 590 Hz at a 4.5-kHz spinning speed.[33] The reduction in the width of the static spectrum upon sample spinning indicates the presence of some residual anisotropic interaction. However, this interaction may be simply due to the difference in the bulk magnetic susceptibility between surface and solid; this effect would be removed by MAS. The weak spinning sidebands of this peak and the relatively sharp nonspinning line width indicate that the anisotropic NMR interactions (chemical shift anisotropy and dipolar coupling) must be greatly reduced by molecular motion that occurs rapidly on the NMR time scale (i.e. with a rate greater than 10^{-4} s). We note that proton exchange alone, although capable of averaging the homonuclear dipolar coupling (ca. 50 kHz) to zero, will not necessarily average the proton chemical shift anisotropy to zero. This can only be effected by motions that change the orientation of a given proton shielding tensor,

(59) Suzuki, M. *Colloq. Int. C.N.R.S.* **1973**, *230*, 77.
(60) Fowler, B. O.; Moreno, E. C.; Brown, W. E. *Arch. Oral. Biol.* **1966**, *11*, 477.
(61) Dry, M. E.; Beebe, R. A. *J. Phys. Chem.* **1960**, *64*, 1300–4.

which is essentially molecule fixed. Since the chemical shift anisotropy for rigid water is approximately 20 ppm (4000 Hz at 200 MHz),[62] the narrow line width and symmetric shape obtained in our nonspinning experiments indicate that the motions of the adsorbed water involve effectively isotropic reorientation of the shielding tensor. It is possible that translational diffusion over the surfaces of the colloidal-dimension crystallites is responsible for the narrow lines; differences in the effectiveness of such motional averaging for different samples might explain the variations in line width for different samples observed here and reported by other workers.[25] All of the adsorbed water must be undergoing such motions, since no evidence for a broad water component has been observed in these apatites.

The ^1H chemical shifts of adsorbed water in HAP and fluorohydroxyapatites are not discussed in terms of hydrogen-bonding strengths since they may be affected by chemical exchange with surface hydroxyl or acid phosphate groups.

Structural Water. The spectra of brushite, gypsum, and OCP reveal characteristic spinning sideband patterns assigned to the structural hydrate water molecules. These spinning sideband patterns resemble the spectral appearance expected for a "Pake doublet" in the slow-spinning limit, as predicted earlier by Maricq and Waugh[43] on the basis of the inhomogeneous character of the dipolar interaction in isolated two-spin systems. In principle, the two hydrogen atoms on a water molecule in crystal hydrates cannot be simply viewed as such a two-spin system, since in addition to the intramolecular H···H interactions there are also sizable intermolecular interactions with neighboring water molecules, which render the total dipolar interaction homogeneous. However, the spectra in Figure 6a,b demonstrate, for the first time by experiment, that fast magic-angle spinning can overcome this latter homogeneous interaction, resulting in spinning sideband patterns that closely resemble those of isolated water molecules. Thus high-resolution ^1H NMR spectra in the solid state can be obtained in these systems without recourse to isotopic dilution or multiple-pulse experiments. At the spinning speeds achieved in the present study (8 kHz) the MAS NMR peaks are still somewhat broad, precluding, for instance, a discrimination of hydrogen-bonding differences occurring for the water molecules of brushite and OCP. This breadth is probably due to incomplete averaging of the intermolecular ^1H–^1H dipolar couplings among neighboring water molecules, a limitation that could be overcome by higher spinning speeds.

It should be pointed out that the homonuclear dipolar coupling in an isolated two-spin system is inhomogeneous in the MAS NMR sense only when the two spins have equal chemical shift tensors with identical orientations.[43] When these orientations are different, as for rigid isolated water molecules, the dipolar interaction becomes homogeneous. In this case, complicated "powder pattern" line shapes result for the central MAS NMR peak, since the chemical shift anisotropy of water molecules is sizable (ca. 10 kHz at a 11.7-T field strength[62]). On the other hand, it is known that the water molecules in many crystal hydrates undergo fast twofold rotations about the bisector axis (180° "flips") at room temperature. This process would render the chemical shift tensor orientations of the two protons equivalent[63] and hence render the intramolecular dipolar coupling inhomogeneous. Furthermore, such flips are effective in reducing the intermolecular dipolar couplings, hence facilitating averaging by magic-angle spinning. It is therefore possible that the high-resolution peak pattern observed at room temperature for the hydrate water in brushite, gypsum, and OCP will disappear at lower temperatures due to the "freezing out" of such flips.

Correlation between the Proton Isotropic Chemical Shift and Hydrogen-Bonding Strength. The downfield shift of the proton resonance in solution induced by hydrogen bonding has been known for a long time. In solids containing hydrogen bonds of more-or-less well-defined geometry, a number of proton chemical shift tensors have been determined by multiple-pulse methods over the past 15 years.[27,62] Although these methods provide all three components of the anisotropic shielding tensor with respect to the crystal-fixed axes, they suffer from the disadvantage of relatively large inaccuracies in the determination of the isotropic chemical shift, which is the trace of this tensor. Thus, Berglund and Vaughan[27] obtained significant scatter in their correlation of the isotropic chemical shift with the O–H···O distance, which is a measure of the hydrogen-bonding strength. They also noted that although theoretical calculations of hydrogen-bonded dimers[32] reproduced the correlation of the isotropic chemical shifts with O–H···O distances reasonably well, the calculated absolute values were about 8 ppm too far upfield. In a subsequent theoretical investigation,[29] this discrepancy was found to be only about 4 ppm, and both theoretical and experimental correlations were approximately linear over the range studied. The authors also noted that although the chemical shift anisotropy is changed more upon hydrogen bonding than is the isotropic shift, a better correlation with hydrogen-bonding strength is observed for the latter. The origin of this correlation seems to lie with the contributions to the chemical shift arising from induced currents on the two neighboring oxygen atoms. These contributions are deshielding for the components of the shielding tensor *perpendicular* to the O–H···O axis and are more influential than the increased shielding produced along the parallel direction.

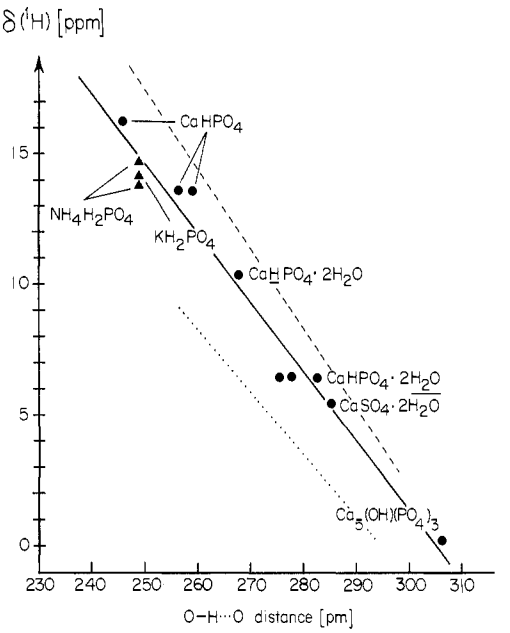

Figure 8. Isotropic ^1H NMR chemical shift (relative to TMS) versus the O–H···O distance in metal phosphates (and gypsum) studied here and reported in the literature.[42,64] The mean of the two O–O distances given for gypsum in ref 68 was used. The solid line represents a linear regression fit to these experimental points. The dashed line represents a linear regression fit to Berglund and Vaughan's data.[27] The dotted line is the corresponding fit to theoretical calculations by Ditchfield and co-workers.[29]

Figure 8 shows the correlation of the isotropic proton chemical shift with the O–H···O distance for the compounds investigated in the present study and for two other metal phosphates reported in the literature.[42,64] We suspect that the reduced scatter compared to the previous linear correlation[29] is due not so much to the fact that only one class of compounds is being considered as to the improved accuracy of the ^1H MAS NMR method. Our least-squares-fit line agrees fairly well with the previous linear correlation, although the slope is slightly less (−0.26 ppm/pm) and closer to the theoretical calculations carried out for hydro-

(62) Haeberlen, U. *High Resolution NMR in Solids*; Academic: New York, 1976; p 149.

(63) McKnett, C. L.; Dybowski, C. R.; Vaughan, R. W. *J. Chem. Phys.* **1975**, *63*, 4578.

(64) Scheler, G.; Haubenreisser, U.; Rosenberger, H. *J. Magn. Reson.* **1981**, *44*, 134.

gen-bonded dimers of RCOOH and ROH.[29] The shift predicted from these calculations is still slightly upfield of the experimental values. Nevertheless, the agreement must be considered very good for an ab initio method, especially since the *absolute* values of the shielding are of the order of 30 ppm, and the calculations were carried out for different hydrogen-bonded systems.

Our results on the fluorohydroxyapatites show that similarly sensitive correlations exist for O–H···F distances. Very slight changes in the hydrogen bonding observed spectroscopically are reflected in the isotropic chemical shifts, supporting the claim that these shifts can be used as accurate diagnostic indices of hydrogen bonding.

We should also note that recently it has been argued[28] that the O···H bond length should be used as a measure of the hydrogen-bond strength, and a linear correlation of this parameter with previously reported isotropic proton chemical shifts was observed. We believe that because of the uncertainties often attendant upon determination of the proton positions in hydrogen bonds, despite improvements in crystallographic techniques, the correlation with the O–H···O distance we have used requires less "adjustment" and provides an equally valid index of hydrogen bonding.

In addition to the influence of hydrogen-bonding strengths, the effect of charge upon the ^1H chemical shift has been studied theoretically for isolated species.[42,65] For the H_3O^+ group the theoretically predicted downfield shift agrees with experimental observations.[42] In contrast, the upfield shift calculated for an isolated OH^- group does not agree with experimental data, including those reported here. This disagreement may result from the fact that, in a crystal lattice, the cations surrounding an OH^- group will tend to reduce the negative charge. More detailed experimental studies of hydroxyl-bearing species would clearly be desirable to clarify the influence of residual charges on chemical shift differences between hydroxyl and water species, apart from hydrogen-bonding effects.

Conclusions

We have shown that fast magic-angle spinning ^1H NMR provides a powerful method for distinguishing and quantitating the various different chemical environments in which hydrogen atoms can occur in crystalline calcium phosphates, including solid solutions. We have also shown that high-speed ^1H MAS NMR yields high-resolution spectra of water molecules in crystal hydrates, with characteristic spinning sideband patterns extending over 100 kHz, due to the largely inhomogeneous character of the strong intramolecular dipolar coupling. Alternative ^1H MAS NMR approaches using deuterium labeling or multiple-pulse line narrowing would eliminate this characteristic spinning sideband signature and thus result in a loss of structural and dynamical information. Indeed, we have used this spinning sideband pattern to identify small amounts of water present in a variety of different minerals.[66]

The variability observed in the relative intensities of peaks in various samples of octacalcium phosphate ($Ca_8H_2(PO_4)_6 \cdot 5H_2O$) reflects positionally disordered hydrogen atoms and suggests a more complex structural chemistry than previously known. In view of the evidence that OCP is a precursor to the formation of defect apatites in mineralized tissue, further NMR investigations of its crystal chemistry and topotactic conversion to hydroxyapatite are clearly important. Preliminary results on mineralized tissue indicate that ^1H MAS NMR will be useful in identifying the calcium phosphate phases present on the basis of isotropic chemical shifts, spinning sideband patterns, and the dependencies of line widths upon spinning speeds.[67]

Acknowledgment. We thank Dr. Sten Samson and Larry Henling for assistance with the X-ray powder diffraction measurements and Jim Hanson for the FT/IR spectra. We are very grateful to Dr. W. E. Brown and his co-workers for providing the latest structural refinement data on OCP prior to publication and for providing several OCP samples. This research was carried out at the Southern California Regional NMR Facility, supported by NSF Grant CHE 84-40137.

(65) Fukui, H.; Miura, K.; Tada, F. *J. Chem. Phys.* **1983**, *79*, 6112. Fukui, H.; Miura, K.; Yamazaki, H.; Nosaka, T. *J. Chem. Phys.* **1985**, *82*, 1410. Rohlfing, C. M.; Allen, L. C.; Ditchfield, R. *Chem. Phys. Lett.* **1982**, *86*, 380.

(66) Yesinowski, J. P.; Eckert, H.; Rossman, G. R. *International Mineralogical Association* Meeting Abstract and *Talk*, *Stanford*, CA, July, 1986. Yesinowski, J. P.; Eckert, H.; Rossman, G. R., submitted for publication.

(67) Yesinowski, J. P.; Evans, J. S., to be submitted for publication.

(68) Cole, W. F.; Lancucki, C. J. *Acta Crystallogr. Sect. B: Struct. Crystallogr. Cryst. Chem.* **1974**, *B30*, 921.